

UCLA

**Adaptive Optics for Extremely Large Telescopes 4 -
Conference Proceedings**

Title

Simulations of AO for the E-ELT and its instruments

Permalink

<https://escholarship.org/uc/item/7kh262xf>

Journal

Adaptive Optics for Extremely Large Telescopes 4 – Conference Proceedings, 1(1)

Author

Le Louarn, Miska

Publication Date

2015

DOI

10.20353/K3T4CP1131713

Peer reviewed

Simulations of AO for the E-ELT and its instruments

Miska Le Louarn^{*a}, Henri Bonnet^a, Michael Esselborn^a, Pierre-Yves Madec^a, Enrico Marchetti^a
^aEuropean Southern Observatory, Karl Schwarzschild strasse 2, D-85748 Garching, Germany

ABSTRACT

We present an overview of the latest simulation results obtained for the European Extremely Large Telescope's different Adaptive Optics systems. Different areas of the telescope and instruments are covered. Simulations showing how a single conjugated AO system can be used to detect a scalloping error is shown. We show that when the scalloping error modes are entered in the reconstruction modal basis, the DM shape can be used to estimate the scalloping error through a simple matrix vector multiply. Temporal averaging allows to get rid of the atmospheric noise on the scalloping measurement assuming a perfect "scalloping actuator" and to get a measurement accuracy of ~ 20 nm rms. In a second part, we focus on a few results obtained on tomographic AO systems, like for example the sensitivity to the number of Deformable Mirrors and their pitch in multi-conjugate AO, and the impact of the outer scale of turbulence on Laser tomography AO.

Keywords: Adaptive Optics, Extremely Large Telescopes, Wavefront sensing, Scalloping, Outer scale of turbulence, Multi-conjugate AO, Laser Tomography AO.

1. THE SCALLOPING ERROR

The scalloping error considered here is a wavefront aberration arising from the compensation by the secondary mirror of the E-ELT telescope ([1]) of a shape deformation of the primary (which is segmented) (see for example [2]). Here, the actual segment shape is fine, they do not need to be warped. It is just that a primary mirror (M1) focus is erroneously compensated by the secondary mirror (M2). Scalloping appears as a high spatial frequency aberration, which can only be partially compensated by the adaptive mirror (M4) integrated into the telescope.

What we want to investigate is whether a turbulence optimized Single Conjugate Adaptive Optics (SCAO) can do something useful on scalloping, when observing through turbulence. There are only ~ 3 actuators and wavefront-sensor sub-apertures per M1-segment, so it is unclear if any useful information on scalloping can be measured through atmospheric turbulence and whether the correction will be efficient.

We start by simulating a simple case: bright NGS, on-axis, static scalloping map.

Figure 1 shows two scalloping modes. Screen001 results from an M1 compensation of a lateral motion of M2. That means on segment scale there is astigmatism as the dominant apparent aberration. Screen002 results from M1 compensation of an axial motion of M2. That means on segment scale there is focus as the dominant apparent aberration.

2. SCAO SYSTEM DESCRIPTION

We describe in this section the SCAO system. It is optimized to correct turbulence, NOT to correct telescope errors like scalloping (unless otherwise noted). This means for example that the sub-aperture field of view and pixel scale are adapted to residual turbulence.

The wavefront sensor model is diffractive, where the shape in each Shack-Hartmann spot is calculated by a Fourier transform of the incoming phase.

The SH sensor has 74×74 sub-apertures (i.e. 50cm projected on M1). The wavefront sensing wavelength is 700nm (monochromatic). FOV / sub-aperture is $2.4''$ (like in NACO, the SCAO system install on the ESO very large telescope VLT), with 4×4 pixels / sub-aperture, atmospheric seeing is $0.8''$. We use an integrator with a gain of 0.3, 3 frames of pure delay (to take into account the relatively slow rise time of the M4 adaptive mirror). The M4 actuator geometry is taken into account, but we neglect here the segmentation of M4 and spiders of the E-ELT. We are operating on-axis, with a high flux on the WFS. The AO system is modeled using Octopus, the ESO AO simulation tool ([3]).

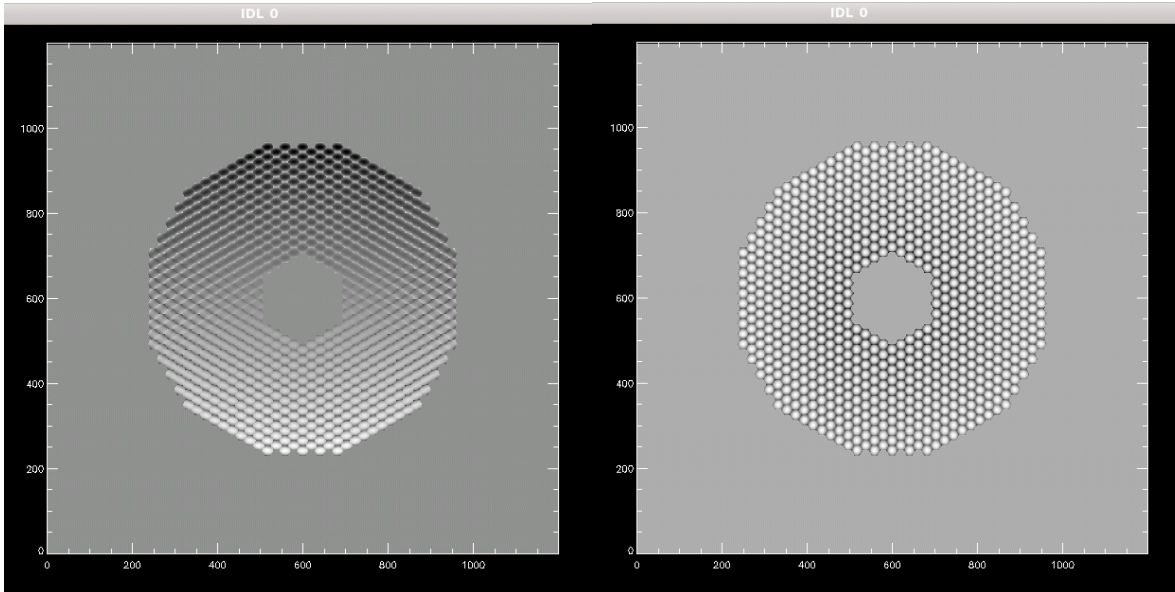


Figure 1: Screen001 (on the left) Screen002 (right), as seen in the AO WFS. Screen 001 corresponds to a lateral shift of M2 compared to M2, Screen 002 corresponds to a radial displacement.

3. FITTING ERROR – M4 MODEL

We now derive the fitting error using the AO simulator. In this case, we find the best M4 shape that fits the scalloping shape, without using a wavefront sensor. This tells us the best correction the M4 can provide with a perfect measurement of the aberrations.

For this, the influence functions of the M4 are used (with 5170 actuators), using the exact geometry of the deformable mirror (including its influence functions). We did not take into account the segmented nature of the M4 (for which the effect on fitting error has been shown to be negligible). We did a least-squares zonal fit of scalloping shape using the FEA simulated IFs and this is what provides the fitting error. We get a fitting error Strehl ratio of 99.94% K band (2.2um), which (using the Maréchal criterion) corresponds to 8 nm rms of wavefront error for screen001. For screen002, 99.68% and 19.6 nm rms.

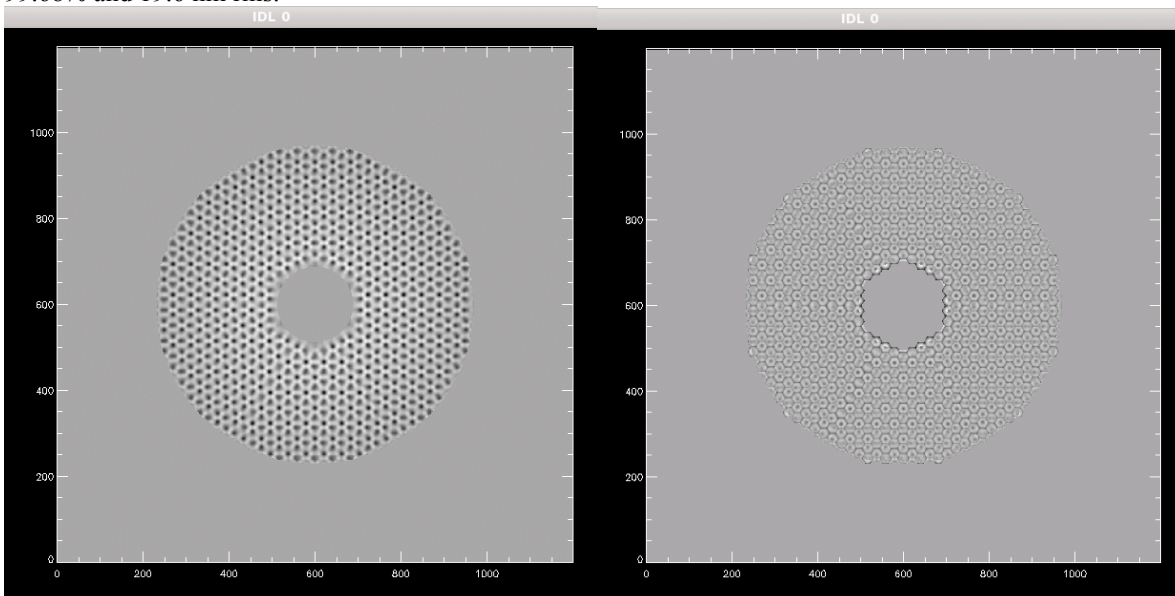


Figure 2: DM shape (on the left) and residual phase after fitting by the M4 (right), for screen002.

We can see that the M4 adaptive mirror has corrected the low order aberrations, but some high order ones remain. We can also see in the residuals the 6-fold symmetry of M4 actuators.

4. CLOSED LOOP WITHOUT TURBULENCE

In this section, we add the SH wavefront sensor to the system. Previously, only fitting error was considered, now also aliasing (i.e. measurement of the aberrations) will be taken into account.

The loop is closed only on Screen001 or Screen002 without atmospheric phase screens, and we see how the WFS/DM combination can correct of the scalloping error. The reconstruction matrix is here the pure atmospheric AO matrix, which hasn't been optimized for scalloping. The results are as follows:

Screen001 → Strehl = 99.80013 % or 15.6nm rms

Screen002 → Strehl = 99.15980 %, or 32 nm rms

We can see a slight degradation of performance compared to fitting error, which was to be expected, as some high frequency aberrations introduce a noise in the wavefront sensing process.

5. RECONSTRUCTION MATRIX INCLUDING SCALLOPING

We now want to tackle scalloping measurement through atmospheric turbulence, in closed loop. In order to estimate the scalloping appearing on the DM, an AO reconstruction matrix taking scalloping into account is calculated. This is done in the following fashion:

- In the AO simulator, Octopus, the shape of the 2 scalloping modes (001 and 002) are added at the end of the Karhunen-Loeve modal reconstruction basis
- The commands to produce each mode (incl. scalloping) is calculated with a least squares fit, using the influence function and actuator geometry of M4. For each mode, there is a set of commands to produce its shape on the DM. Therefore, we have a matrix ($N_{\text{modes}} * N_{\text{commands}}$).
- This matrix is inverted, to obtain a modal projection matrix (called Z) which gives, for a set of DM commands, the modal coefficient for each controlled mode. This matrix does a full reconstruction over all the controlled modes. Because 001 and 002 are the last modes controlled, their coefficients are the last in the reconstruction matrix.
- The AO reconstruction matrix is calculated "as usual" using MAP, but with the scalloping modes replacing the last two KL modes (usually numbers 5001 and 5002 is 5000 atmospheric modes are controlled). We use a MAP method for this, which includes a turbulence covariance matrix. This allows to give each mode its energy in the atmosphere, and this influences the gain of this mode in the AO command. So for example, tilt has a high energy in the atmosphere, and therefore it has a high gain in the command. For scalloping, we have used the atmospheric covariance of the last 2 KL modes. This is clearly not optimal, and should be optimized in the future.

This method allows to force the system to do a global fit (using 5000 KL modes, and 2 scalloping modes). It does not just fit scalloping, but all the controlled modes in addition, at the same time. This allows disentangle efficiently scalloping from other (atmospheric) perturbations.

6. CLOSING THE SCALLOPING LOOP

In order to close the scalloping loop, during the AO closed loop, the following is done:

- Octopus starts with a phase screen composed of scalloping (the default, unless otherwise mentioned, is $\text{Phase} = 10 * \text{Phase}(001) - 10 * \text{Phase}(002)$), in addition to the turbulence phase screens. $\text{Phase}(001)$ and $\text{Phase}(002)$ are the shapes of Scalloping001 and Scalloping002 in phase space. This is quite a large amplitude (to test robustness of the method at startup), which reduces the Strehl ratio significantly. The WFS sees therefore turbulence + scalloping. The idea is to look at the robustness of the system, and therefore a large amount of both scallopings is injected, simultaneously.
- At each AO loop iteration, the DM commands (c, vector of full commands, after integrator) are stored
- After 100 AO iterations (the AO is running at 500Hz, so this is 0.2s), the DM commands are analysed by an independent script, which calculates for each time step: $S = Z \# c$ for each command. S is a vector of modal coefficients, for which the last values represent modes 001 and 002.
- The average of S over the 100 iterations is calculated for each mode.

- A new shape for the scalloping screen sent to Octopus is calculated, using S and a gain: $\text{New_phase} = \text{Phase} - \text{gain} * (S(001) * \text{Phase}(001)) - \text{gain} * (S(002) * \text{Phase}(002))$. Where $S(001)$ and $S(002)$ are the coefficients for the two scalloping.
- After the first 100 iteration of the AO loop, the scalloping correction is applied with a very high gain, of 0.95. In the following scalloping iterations, a much lower gain (between 0.05 and 0.6, default is 0.2) is applied. This is to reduce the number of simulation iterations necessary to obtain convergence.
- New_phase is sent to Octopus, as the new screen to be applied. With this scheme, we simulate a perfect “scalloping actuator”, capable of perfectly removing the scalloping, once it is detected.
- In a perfect world ($M4$ commands provide a perfect measurement of scalloping), New_phase would tend towards zero (no scalloping is sent to Octopus, as all scalloping is seen and perfectly corrected). This is of course not the case, since turbulence is introduced in the WFS:ing process (atmospheric “noise” – due to the projection of the atmosphere on scalloping, plus aliasing of high orders in the WFS measurement).

The control loop schematic of the algorithm is shown below – indicating where the scalloping signal is injected into the system:

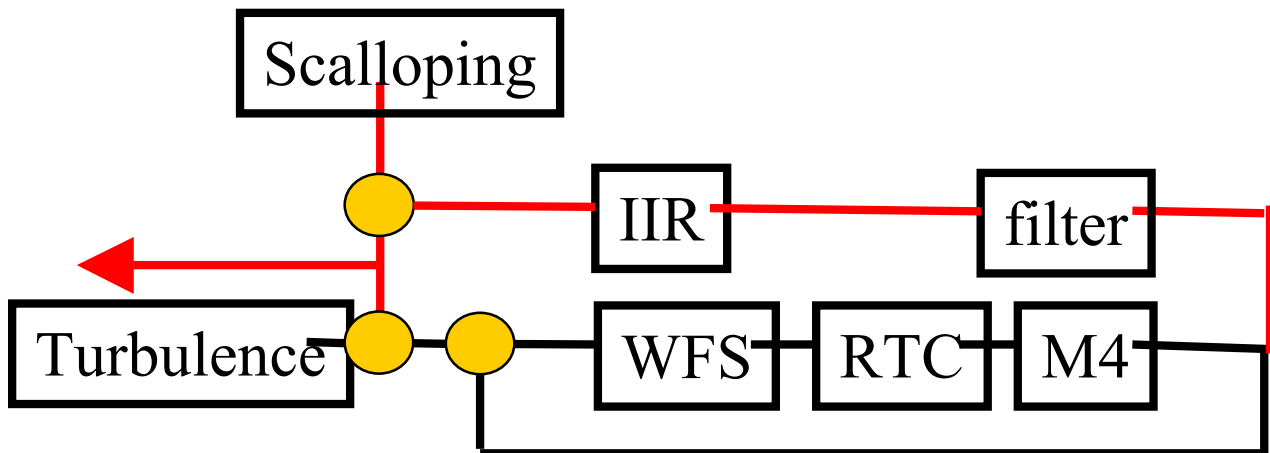


Figure 3: Schematic representation of the scalloping loop. The grey lines are the AO loop, the red lines the scalloping part. The red arrow represents the tap point for the scalloping residuals.

The following plot (Figure 4) shows the Strehl ratio (on axis, K-band) as a function of time (AO loop). We can see at the beginning, that the Strehl increases as the AO loop is closed (atmosphere is corrected), but stays stuck below 20%. This is because the $M4$ cannot, by itself, correct the very large amount of scalloping (and the aliasing it causes) that has been injected very well. It does something useful though, and therefore there is an improvement at the beginning.

After 0.2s, the first scalloping correction command is sent. First the AO system Strehl is reduced (!). This is because suddenly, there is much less scalloping (since it has been perfectly corrected by the scalloping actuator), BUT the DM still corrects it from the previous measurement of scalloping. Then, the Strehl very quickly increases, as the scalloping is removed from the DM by the AO loop.

The other corrections of scalloping (every 0.2s) are not anymore visible, although they occur. This demonstrates that in the principle, scalloping correction from $M4$ data works, in this idealized (bright on-axis NGS, in a SCAO system, ideal scalloping actuator) case.

Now, we want to know how efficient this scalloping correction is. For this, we look at the commands (which are actually residuals which should tend to zero) that are sent back to Octopus from the scalloping measurement. These residuals show how much turbulence affects (due to measuring scalloping (and the projection of turbulence on it) from $M4$ scalloping measurements).

The following figure shows the amplitude (nm rms) of the scalloping command (i.e. scalloping residual) sent to Octopus as a function of time (correction rate of AO loop framerate divided by 100, i.e. 5Hz).

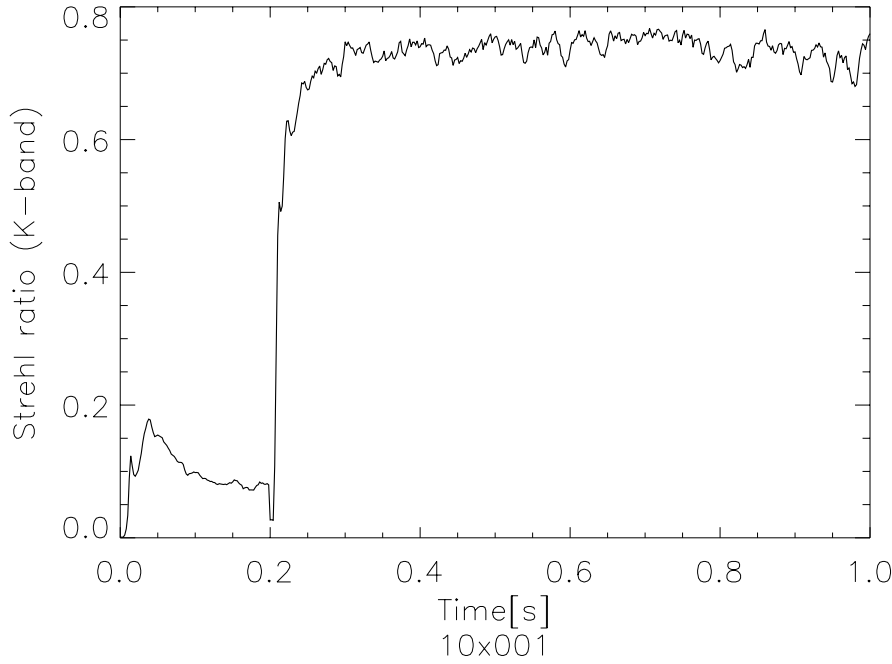


Figure 4: Time series of the AO loop closing in presence of scalloping (here, starting with 10×001). This is the Short exposure K-band Strehl ratio, the Long Exposure Strehl at 1.0s is $\sim 70.56\%$.

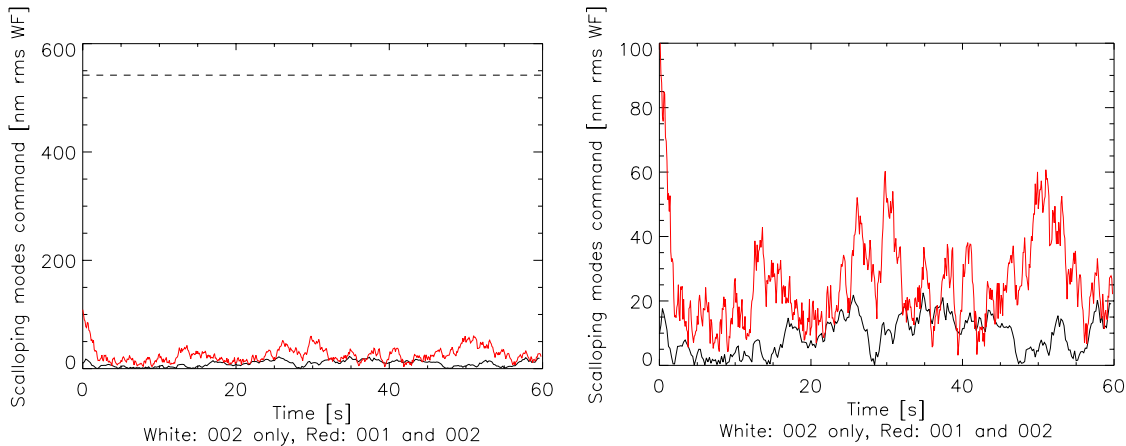


Figure 5: Scalloping residuals as a function of time (in nm rms). The dashed line shows the original input value. Black line is when only 10×002 is sent at the beginning and only mode 002 is corrected (other mode has a gain of zero). The red curve is when $10 \times 001 - 10 \times 002$ is introduced and both modes corrected. On the right, is a zoom of the same curve as on the left.

From the previous curves, we can see that most of the initial (large) scalloping is corrected immediately (because we use the very high 0.95 gain at the first iteration). After that, the scalloping residuals stay relatively constant with time.

We note that correcting the two scalloping (001 and 002) degrades the performance compared to only correcting 002. Indeed, in the first case, we have 23 nm rms of residual, while in the second case, this is reduced to 11 nm rms. The reason for this is probably the atmospheric component's projection on the scalloping modes. Having two scalloping modes allows more turbulence to project into the correction than only one.

We have verified that the input scalloping (in the phase space) modes are orthogonal, by looking at their scalar product, which is $2.1 \cdot 10^{-5}$. However, it is not guaranteed that they remain orthogonal in the control space (as seen by the WFS and processed through the reconstruction matrix).

It may be possible to orthogonalize the basis in the controlled space, to improve performance when the two modes are corrected. But then, we would not be sure that one can easily send commands in the 001 and 002 modes defined in the phase space.

6.1 Scalping loop gain

Next, we investigate the performance of the scalping correction as a function of the scalping loop gain. The results are seen for two different correction frame rates (5 Hz in solid and 10Hz in black) in the following plot:

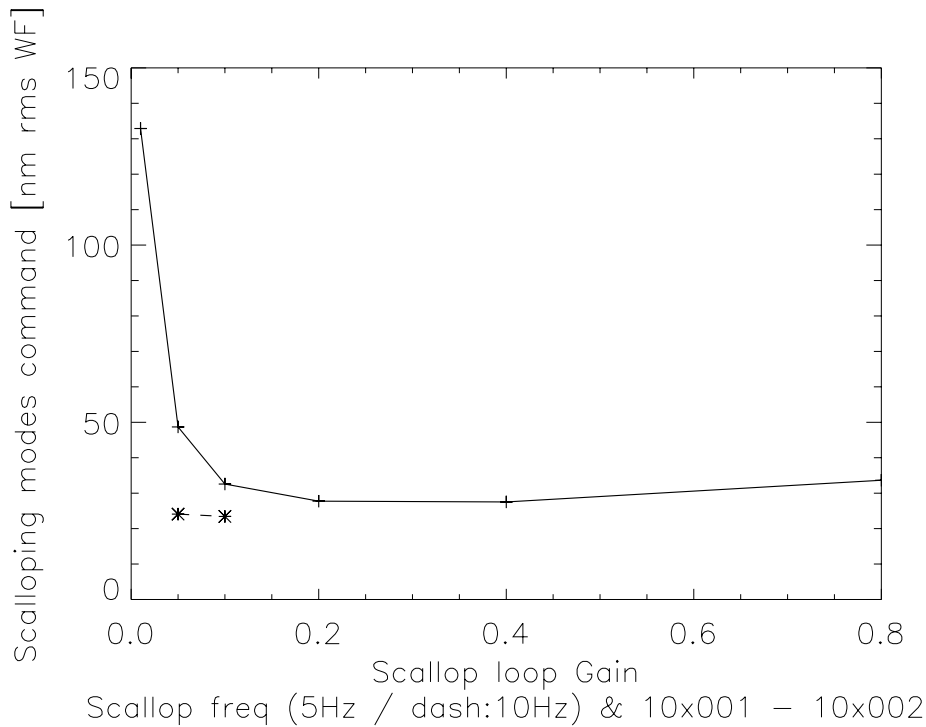


Figure 6: Scalping residuals (averaged between $t=10s$ to $t=60s$) as a function of scalping loop gain. The solid curve is for 5Hz, the dashed on for 10Hz.

With gain 0.1, every 50it (10 Hz), we get the median scalping residual of 23 nm rms.

Since most of the error is likely residual atmospheric turbulence, this curve is a bit perplexing. A lower gain means a longer integration time on turbulence, and therefore a better averaging out of the turbulence. It is possible that other errors (due to the length of the simulation, size of the phase screens, direction of phase screen shifting) contribute to this curve. Indeed, we are already doing quite a lot of averaging at 0.2, 5Hz or 10Hz, and we cannot be certain of the complete averaging out of the turbulence in the simulation. More testing with larger / more phase screens at different speeds are needed.

6.2 Response on scalping only

So what happens when the atmosphere is removed from the system, if we only try to correct the scalping? Nothing is changed in the system, except all the atmospheric phase screens are put to zero.

We can see the previous behaviour, (low Strehl until first scalping command is sent, then significant improvement in Strehl). What happens afterwards is not yet well understood. The oscillations that appear after about 0.6s are probably due to the fact that the SH is not dimensioned to correct only scalping (the pixels are too big for the spot size – which is now much smaller, since there is no turbulence). The oscillation could possibly be reduced by reducing the AO loop gain, or reducing the size of the Shack-Hartmann pixels (or increasing the spot size by putting a calibration fiber). We could also try to optimize the AO command matrix for the non turbulent case.

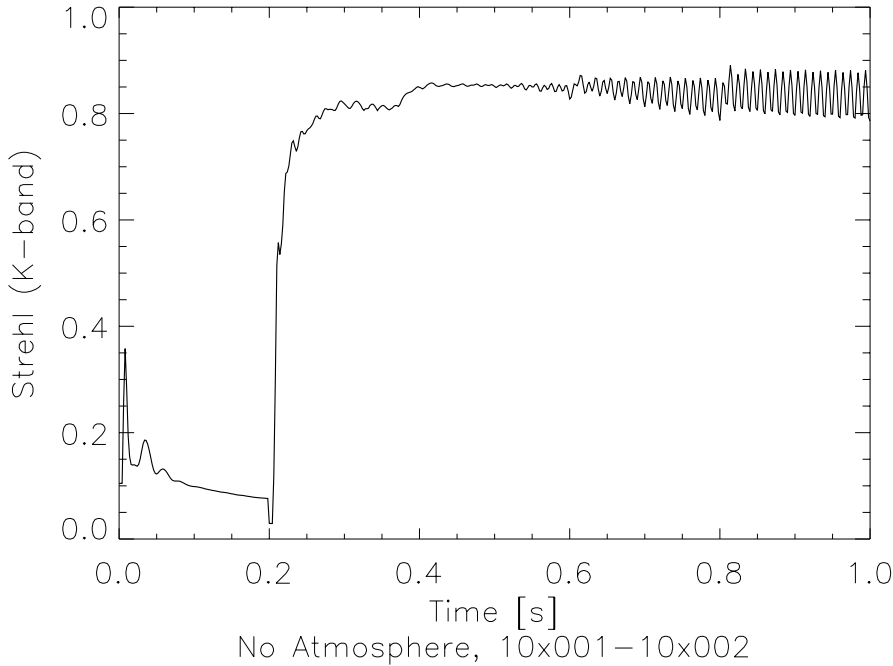


Figure 7: AO closed loop, with the default amount of input scalloping, when there is no atmosphere. This is the Short exposure Strehl

6.3 Response without scalloping

The next question is to see what happens to the system, when no scalloping is introduced, but it is still corrected. It is a way to see how stable the system is, and how atmospheric turbulence residuals after averaging and measurement errors (aliasing in the WFS) propagates into the scalloping correction. We get a long exposure (integrated) Strehl ratio of 71.01% after 5000 AO iterations.

This is to be compared with the case where the scalloping loop is run with a gain of zero (where it cannot perturb the AO system). In that case we see a long exposure (integrated) Strehl ratio (after 5000 AO iterations) of 71.07%. This shows that the scalloping loop does not perturb the AO performance significantly (in the case no scalloping would be introduced by the system).

Below, we show the scalloping residuals without any scalloping injected at the beginning of the AO loop. This shows how the measurement errors are injected as scalloping into the system. Note how similar this curve is to Figure 5. We can see that we are mostly dominated by the measurement errors (likely the atmosphere).

When there is no scalloping introduced initially, we get 23.7 nm rms residual after 60s of simulation, very close to the result with scalloping. This tends to show that most of the error is due to the atmospheric residuals. Getting rid of those residuals will likely require more temporal averaging. Note that this atmospheric component will impact all scalloping measurement methods, not just when using M4 (a specific scalloping sensor would also have to reject turbulence through averaging).

In the next sections, we move toward a very different subject. We are not concerned with scalloping anymore and investigate the performance various tomographic AO systems (looking through turbulence), and in particular, look at their sensitivity to various effects.

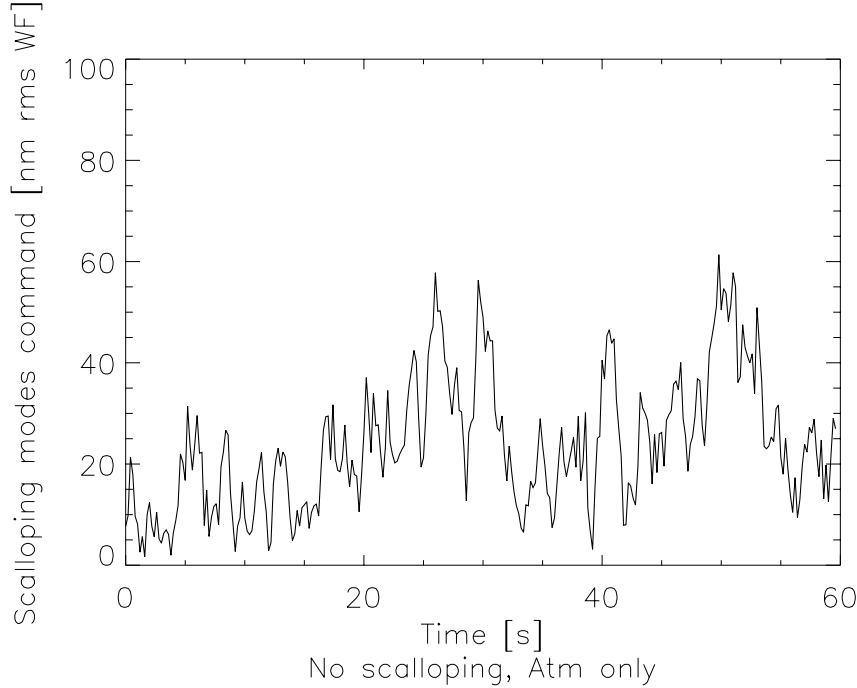


Figure 8: Scalloping coefficient (residual) as a function of time, when there is no scalloping initially.

7. TOMOGRAPHIC AO SENSITIVITY ANALYSIS

Simulations have been carried out to understand the sensitivity of Laser Tomography AO and Multi-Conjugate AO to different parameters. In this section, we will present the results for the sensitivity of MCAO ([5]) to the Number of high altitude deformable mirrors, actuator density on them and also to the profile in height of the outer scale of turbulence. In the following section, for LTAO (see [4]), we have investigated the position of the Laser Guide Stars, related to the Zenith angle of the observations.

For both LTAO and MCAO, we consider: 74x74 subapertures, 6 LGSs (2' diameter constellation in a circle for MCAO, variable diameter for LTAO), no LGS spot elongation, 500Hz frame-rate, seeing~0.8'', Frim3D tomographic reconstruction, 35 layers of atmospheric turbulence ([8]) with 0.8'' seeing (at zenith). Both these AO systems use the adaptive M4 as a corrective element (spacing ~50cm, projected on the pupil, assumed to be conjugated at 0m).

7.1 Multi-conjugate AO

Here, we investigate the performance for different number of deformable mirrors (1 or 2, in addition to M4 which is always used). In case of 1 post-focal DM, its conjugation height is fixed at 10km (which is roughly optimal). In case of 2 post-focal DMs, their heights are 4.5km and 12.7km (also roughly optimal, considering the 35 layer atmospheric model used here). In all cases, the M4 is assumed to be conjugated to 0m. We can see the results in **Figure 9**. The plots show performance as a function of position in the field of view (the MCAO serves to correct a field of view larger than the isoplanatic patch, so performance evolution in the field is of interest). Three series of points are plotted: in Black, 3 DMs (total), with a pitch of 0.5 (ground), 1m (4.5km), and 1m (12.7km). In red, 2 DMs, with pitches of 0.5 (ground), 1m (10km), and blue with 2 DMs, with pitches of 0.5 (ground), 0.5m (10km). We can see that the third DM adds a non-negligible amount of correction all over the field. However, 2 DMs (total) still provides a good quality correction. In all cases, having a lower pitch (1m) on the altitude DM seems an acceptable solution.

The second plot (**Figure 9**, right) compares three cases with a total of 3DMs, with different pitches: in black, 0.5 (ground), 1m (4.5km), and 1m (12.7km), in red, 0.5 (ground), 1m (4.5km), and 0.5m (12.7km) and finally in yellow, 0.5 (ground), 1.5m (4.5km), and 1.5m (12.7km). Here, differences are minimal, and therefore for the simulated conditions, it

seems reasonable to reduce the pitch of the altitude DMs to 1m, or perhaps even 1.5m. Note however, that here we have studied the case with a reasonable good seeing ($0.8''$), at zenith. Going for worse seeings / off-zenith may change these conclusions.

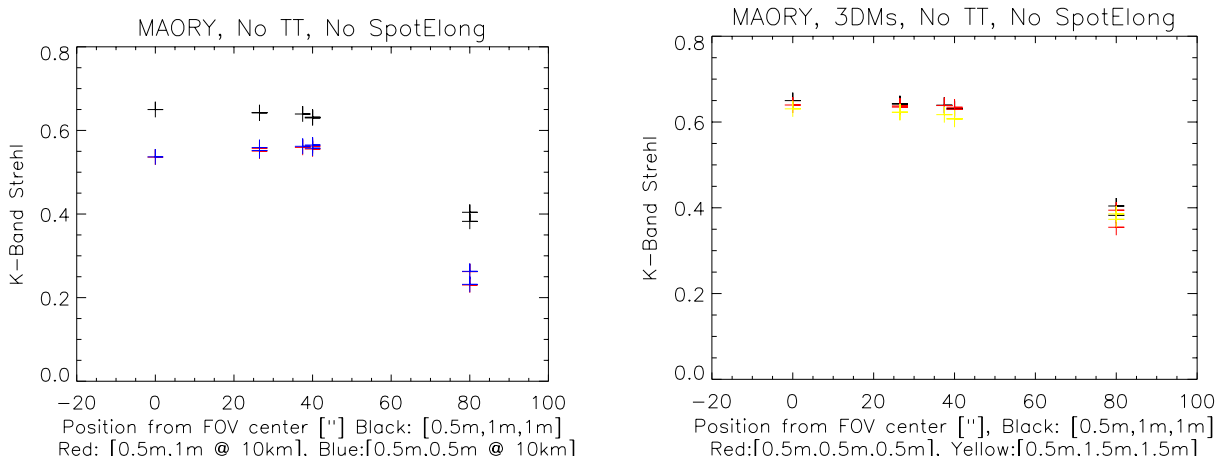


Figure 9: MCAO number of DMs & pitch. On the left, Number of DMs & pitch. On the right, for 3 DMs, impact of the pitch of the DMs.

In the next figures, we investigate another effect, i.e. what happens, when the outer scale of turbulence (L_0) profile with height is changed. In the baseline case (used throughout this paper), $L_0(h) = 25m$, for all heights. Measurements of L_0 , and indeed $L_0(h)$ are scarce. However, DaliAli et al. (2010, ([7]) provide measurements. Here, we use an average $L_0(h)$ profile, where all the profiles of that paper are averaged. This average profile (and quantification for our 35-layer turbulence profile) is presented in **Figure 11**.

Using this $L_0(h)$ profile, we ran some simulations of MCAO performance (using the baseline 3 DMs with 0.5m pitch) simulations. Here, we only look at the central (on-axis) and average over the field Strehl ratios. Two kinds of simulations were run: $L_0(h) = \text{constant}$, and $L_0(h)$ is the profile presented in **Figure 11**. The results can be seen below:

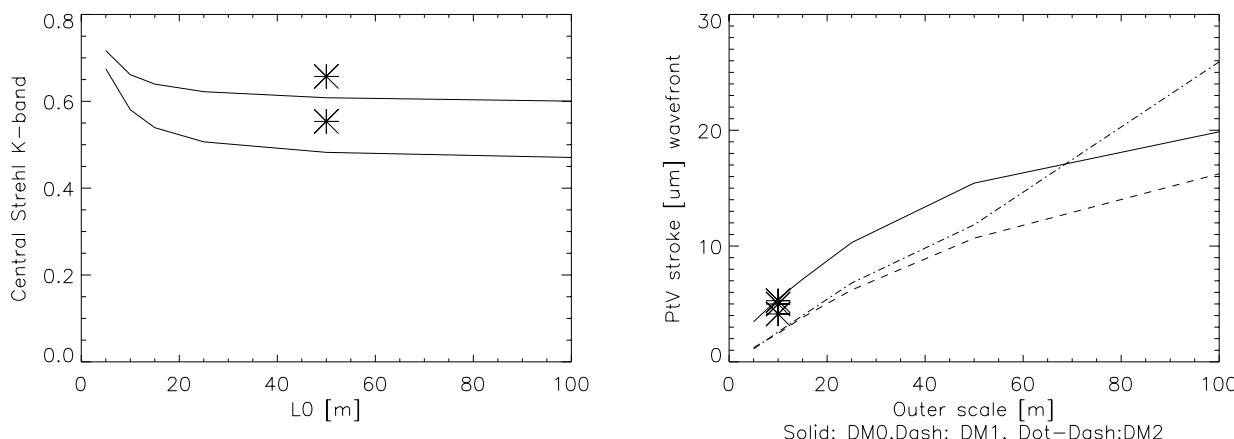


Figure 10: On the left, MCAO performance (on-axis on top, and median of field at the bottom) as a function of outer scale. The Stars represent the cases with the $L_0(h)$ profile of Figure 11. The lines are for $L_0(h) = \text{constant}$ (represented on the X axis). On the right, the peak-to valley stroke (wavefront) over the whole mirror (tip-tilt included) for the different cases (PtV stroke was measured by simply taking the min-max of the DM surface).

In particular, the stroke results show (a well known) strong dependence of the required DM stroke as a function of outer scale. This is not surprising. However, we can note that the $L_0(h)$ profile of Dali Ali et al is very conservative. This has a huge impact on DM stroke. Therefore, if this is a critical parameter, more measurements would be welcome to refine these results.

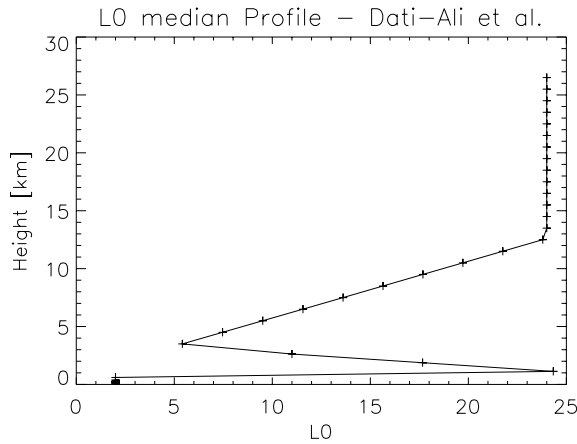


Figure 11: Average L0 profile, obtained by averaging all the DaliAli et al. 2010 L0(h) profiles ([7]). This average profile has been re-sampled for our 35 layer turbulence profile.

7.2 Laser Tomography AO

Finally, a series of simulations was run to look at the performance of LTAO (single DM, i.e. M4, conjugated to the ground), when the zenith angle is changed. This has the effect of making the r_0 worse, but also to increase the height of the LGSs. This in term improves the tomography, the LGSs look more and more like NGSs (from the cone effect point of view) as one increases the zenith angle. At an airmass of 2, the LGSs are at 180km, instead of 90km. This explains why on the curve below, the optimal position of the LGSs gets closer to on-axis. Indeed, if the LGSs were at infinity, they would all be optimally placed on-axis, and would effectively be a single NGS.

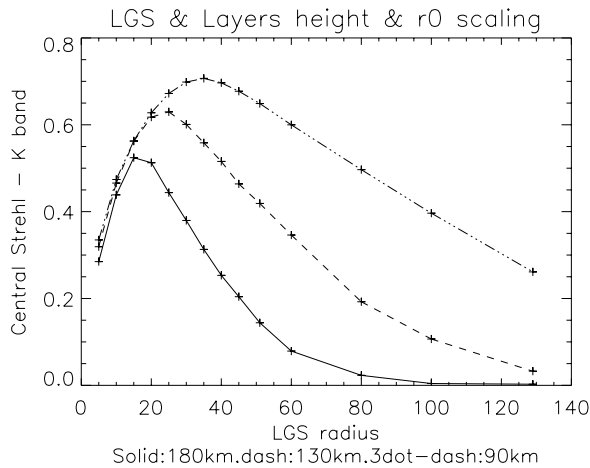


Figure 12: LTAO performance for 3 different zenith angles (0, 30 and 60 degrees). The corresponding LGS heights are at 90km, 130km and 180km, respectively.

Further analysis of this results will be presented in Neichel et al ([6]).

8. CONCLUSIONS

In this paper, we have shown that correcting scalloping using a signal from the deformable mirror commands is possible, in the simplified case we studied (high flux SCAO, on-axis). This requires only a slight adjustment to the command matrix of the AO system, to get a clean signal directly from the commands. The precision of the measurement and correction, in our idealized case is about 23nm rms. The limiting factors are (at least) : atmospheric noise and aliasing. There are outstanding questions: what limits the precision of the correction (probably the atmospheric turbulence residuals) and how to improve, sensitivity to noise, robustness. We also did not study the impact of the actual

conjugation height of the M4 deformable mirror (~600m), nor what happens if scalloping is observed from one (or more) guide stars off-axis.

In addition to the scalloping analysis, we have studied how deformable mirror pitch and number of DMs impact the performance of an MCAO system on the E-ELT. We can say that the pitch of the high altitude DM(s) can probably be relaxed to at least 1m (projected on the pupil). A third DM (total) adds some performance, but a 2 DMs (total) system still provides meaningful correction (but this is before the full error budget, and in K-band). The impact of the outer scale of turbulence (and its profile) was also analyzed, and shows a significant impact on the required stroke of the DMs.

Finally, LTAO performance impact of zenith angle on optimal LGS position in LTAO. We show that larger zenith angles push the optimal LGS position towards smaller angles.

REFERENCES

- [1] https://www.eso.org/sci/facilities/eelt/docs/e-elt_constrproposal.pdf
- [2] Douglas G. MacMynowski, Lewis C. Roberts, J. Chris Shelton, Gary Chanan, and Henri Bonnet, "In-plane effects on segmented-mirror control," *Appl.Opt.* 51, 1929-1938 (2012)
- [3] Le Louarn et al., Trends in AO simulations @ ESO: or 10+ years of Octopus, Modeling and Simulation for Adaptive Optics workshop 2014, http://www.dur.ac.uk/resources/cfai/sim2014/MiskaDurham_presentation_2.ppt
- [4] Neichel et al., The AO modes for HARMONI: from classical to Laser-assisted tomographic AO systems, AO4ELT4, these proceedings.
- [5] Diolaiti et al., The MAORY first-light adaptive optics module for E-ELT
- [6] Neichel et al., in preparation
- [7] Dali Ali et al, Multi-instrument measurement campaign at Paranal in 2007, *A&A* (2010)
- [8] Sarazin et al., Defining reference turbulence profiles for E-ELT AO performance simulations, AO4ELT3, (2012)